

EVALUATION OF BOND BEHAVIOR AT THE INTERFACE BETWEEN TWO DIFFERENT CONCRETES

S. Kono, S. Tsuruda, and T. Kaku,
Architecture and Civil Engineering Department,
Toyoashi University of Technology, Toyoashi, Japan

Abstract

Bond performance of a deformed steel bar lying at the interface between old and new concretes was examined using both experimental and numerical procedures. In the experimental study, fifty-seven Schmidt-Thrö type specimens were tested to study the influence of concrete strength (30 MPa - 100 MPa) and interface conditions on the side split type bond behavior. In a numerical study, specimens were modeled using a smeared crack model and the fracture process simulated. Maximum bond stresses close to the experimental results were predicted for different specimens except for monolithic specimens with concrete strengths higher than 70 MPa.

Key words: Bond, interface, retrofit, high strength concrete

1 Introduction

Deteriorated concrete columns are often retrofitted by replacing old cover concrete with stronger cover concrete. However, the longitudinal reinforcing bars then lie at the interface between the original core and the new cover concrete. Although the bond performance of the longitudinal bars at the interface can be expected to differ from that in the monolithic concrete, its performance has not been evaluated quantitatively. At Toyoashi Univer-

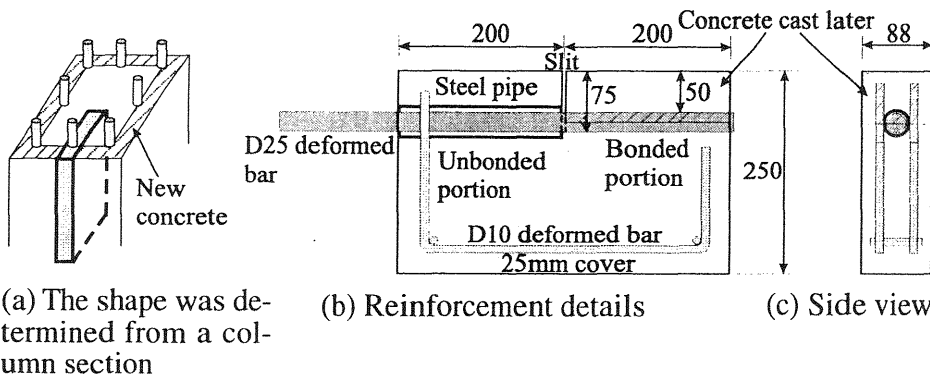


Fig. 1. Schmidt-Thrö type specimen

sity of Technology, experimental studies of bond performance have been made using Schmidt-Thrö type specimens since they are easy to manufacture and test. Unfortunately, however, the mechanism of bond at the interface was not clearly established from those experiments.

In this study, both experimental and numerical approaches were taken to understand the mechanism of bond at the interface from the fracture mechanics view point. In the experimental phase, fifty-seven Schmidt-Thrö type specimens were tested to study the influence of interface conditions and concrete strength ranging from 30 MPa to 100 MPa on the side split type bond behavior. While the maximum bond stress was obtained, the relative displacement between a reinforcing bar and the surrounding concrete was not satisfactorily measured. In the numerical phase, the fracture process at the interface was simulated using the smeared crack model originally proposed by Dahlblom et al. (1990) and subsequently developed by Uchida et al. (1993).

2 Experimental study

2.1 Specimens

The geometry of Schmidt-Thrö type specimens is shown in Fig. 1. Specimens with an interface consisted of two types of concrete; original concrete shown in white and concrete cast later shown as hatched. Monolithic specimens, of course, had only one type of concrete. The specimen was 400 mm long, 250 mm tall, and 88 mm wide and had a 2 mm wide and 75 mm deep slit at the top center. The right side of the slit was the test region. A high strength deformed steel bar of 25 mm diameter (called D25 bar hereafter) was embedded at the interface. Its upper half perimeter contacted concrete cast later if any and the lower half contacted the original concrete. On the left side of the slit, the D25 bar was encased in a steel pipe of 32 mm diameter in order to eliminate bond with the surrounding concrete. In this man-

Table 1. Test variables and results

Specimen type	Test variables		Treatment of interface	Test results		
	Nominal concrete strength(MPa)			Bond strength (MPa)		
	Orig.	New		No. 1	No. 2	No. 3
30-30M	30	30	Monolithic	3.36	3.35	3.38
30-30P			Plain	2.33	2.25	(1.14)
30-30R			Rough	2.44	2.81	3.31
30-45P		45	Plain	2.38	2.37	2.07
30-45R			Rough	2.73	2.80	3.02
45-45M			Monolithic	3.75	4.50	4.09
45-45P	45	45	Plain	2.38	2.31	(1.69)
45-45R			Rough	3.44	2.95	4.03
45-70P			70	Plain	2.01	1.68
45-70R		Rough		3.69	3.70	2.90
45-100P		100		Plain	2.73	2.03
45-100R			Rough	4.34	3.43	2.99
70-70M	70		70	Monolithic	7.32	7.49
70-70P		Plain		3.50	2.19	2.65
70-70R		Rough		3.92	4.40	3.72
70-100P		100	Plain	2.57	2.84	(1.60)
70-100R			Rough	4.50	4.04	4.25
100-100M			100	100	Monolithic	7.76
100-100P	Plain	(3.19)			-	-
100-100R	Rough	(3.36)			(3.47)	-

Due to failure outside the test region and other unknown reasons, bond strength shown in parentheses is considered to be lower than the potential strength.

ner, by pulling the D25 bar to the left, a side split failure was expected only on the right side of the slit.

Test variables were compressive concrete strength and interface conditions as shown in Table 1. There were eight combinations for concrete strength of the original and the new concrete. The numbers before and after the hyphen in specimen types indicate the nominal concrete strength in MPa of the original and the new concrete, respectively. The strength of the new concrete was made equal to, or greater than that of the original concrete since that is customary in practical retrofitting. The letter in the specimen type indicates the interface condition: 'M' stands for monolithic; 'P' for plain interface; and 'R' for rough interface. For R and P type specimens, after the original concrete was cast the specimens were cured in water for 4 weeks. For R type specimens the interface surface was brushed until the aggregates were completely exposed. For P type specimens, no treatment was applied to the interface. For both specimen types, new concrete was then cast on top of the original concrete and the specimens were again cured in water for another four weeks. M type specimens were cast at the same time as the original concrete for P and R type specimens and cured in water for eight weeks. By combining concrete strength and interface conditions,

Table 2. Properties of concrete

	Nominal Strength (MPa)	Compressive strength (MPa)	Tensile strength* ¹ (MPa)	Young's modulus* ² (GPa)
Original concrete	30	26.8	2.81	24.9
	45	44.0	3.66	29.2
	70	76.5	4.86	33.5
	100	100.6	6.63	37.0
New concrete	30	29.5	2.77	22.5
	45	47.2	3.57	31.7
	70	71.6	4.20	33.7
	100	101.0	5.96	39.3

*1: Based on cylinder splitting tests

*2: One-third secant modulus

Table 3. Properties of steel

Steel type	Yield strength (MPa)	Tensile strength (MPa)	Young's modulus (GPa)
D25	1000* ¹	1080	203
D10	347	507	186

*1: Based on 0.2 % offset value

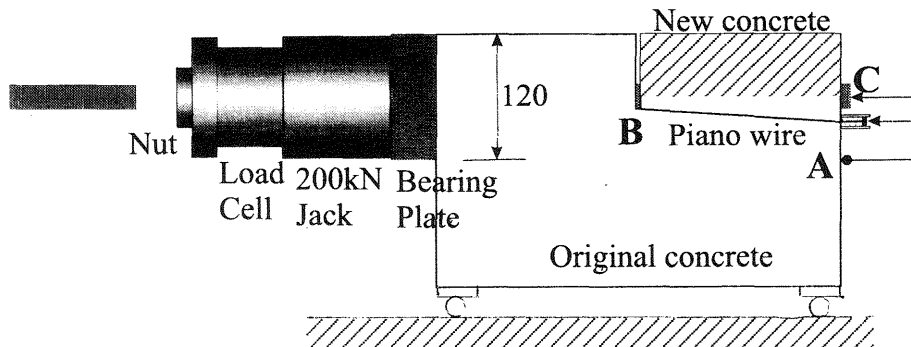


Fig. 2. Loading system

twenty specimen types were prepared. Each specimen type had basically three identical specimens and a total 57 specimens were tested. The mechanical properties of the concrete and steel are shown in Tables 2 and 3, respectively.

The loading system is shown in Fig. 2. The D25 bar was pulled by a center hole jack and the load was measured by a load cell next to the jack. Two rollers were placed under the specimen to eliminate horizontal constraints. The relative horizontal displacement of the D25 bar was measured between A and B and between A and C. The displacement at B was recorded on the right side of the specimen using a piano wire encased in a hard plastic tube.

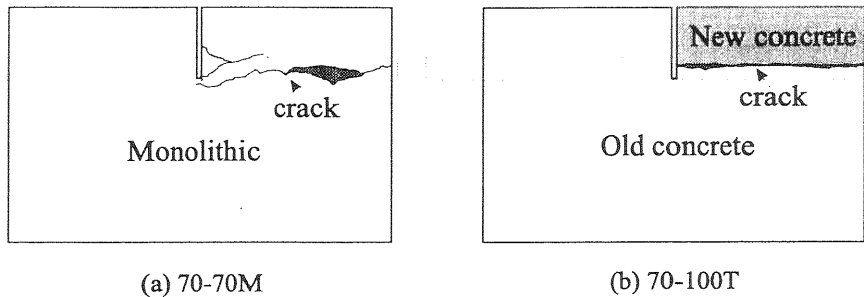


Fig. 3. Representative crack patterns

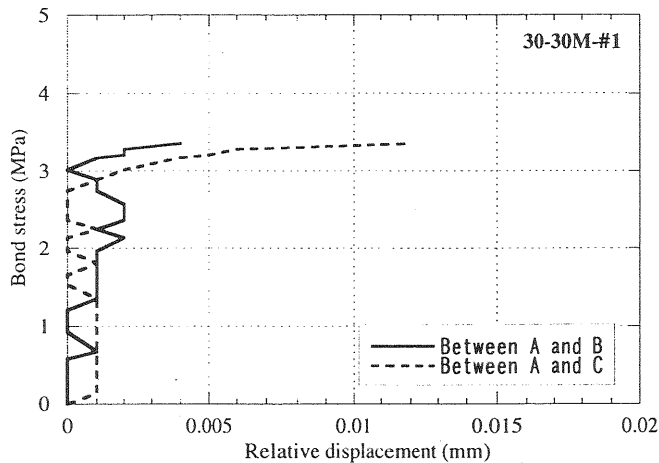


Fig. 4. Bond stress and slip relations in experiment

2.3 Experimental results

Failure modes for the specimens are shown in Fig. 3. In Fig. 3(b), Specimen 70-100R-#1 shows a crack along the interface. However, Specimen 70-70M-#1 in Fig. 3(a) shows multiple tortuous cracks along the D25 bar. The behavior for 70-70M-#1 was typical of M type specimens and that of 70-100R-#1 was typical of P and R type specimens.

The displacement and bond stress relations for 30-30M-#1 are shown in Fig. 4. The resolution of the displacement gage was 0.0005 mm but the results do not show that the prescribed resolution was achieved. Since relative displacements obtained from the other specimens were similar to the results in Fig. 4, the displacement data were discarded.

The bond strength for each specimen is shown in Table 1. The bond

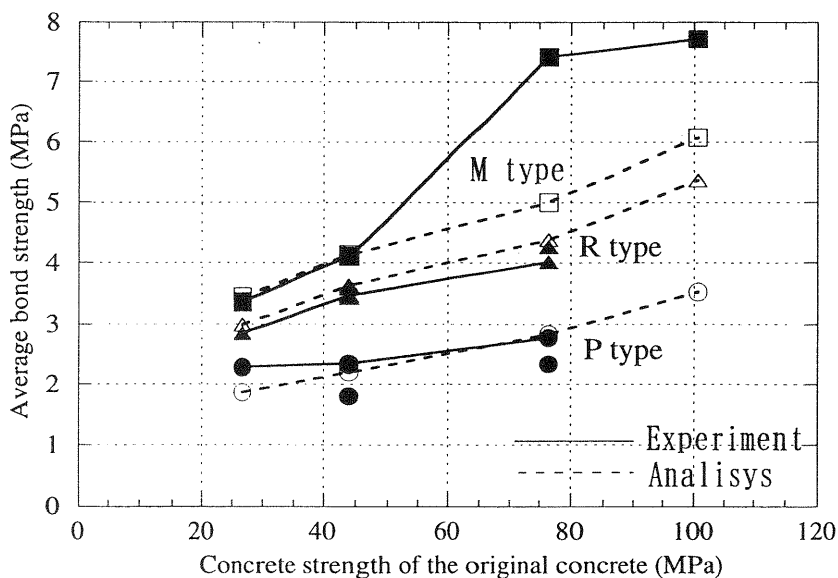


Fig. 5. Bond strength and concrete strength relations

strength was calculated by dividing the maximum tensile force by the contact area of the steel bar whose perimeter was 80 mm and bond length was 200 mm. The numbers in parentheses are considered to be lower than the potential strength and are eliminated from the following discussion because the specimen either failed outside the test region or for some other reason. In Fig. 5, the relations between the average bond strength for each specimen type and the concrete strength of the original concrete are shown. The three different solid symbols indicate experimental results for different interface conditions. Test points are connected by solid lines if the interface conditions are same and the nominal strength for the new concrete is same as that of the original concrete. It can be seen that the average bond strengths were very close if the interface condition and the strength of the original concrete were identical even if the strength of the new concrete was different. This result indicates that the strength of the weaker concrete controls the bond strength. It should also be noted that bond strengths for monolithic (M type) specimens increase rapidly for concrete strengths more than 70 MPa.

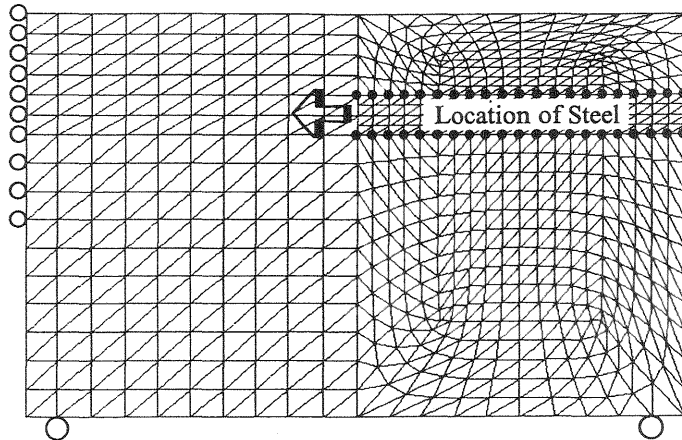


Fig. 6. Mesh used in the analysis

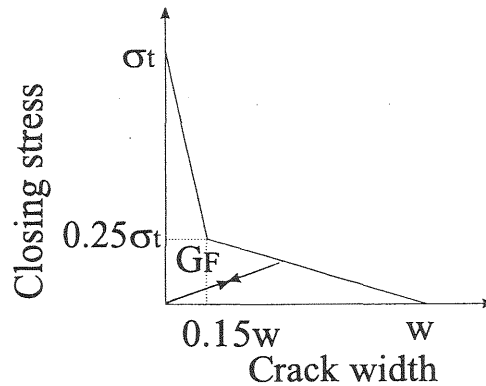


Fig. 7. Relation between closing stress and crack width

3. Numerical study

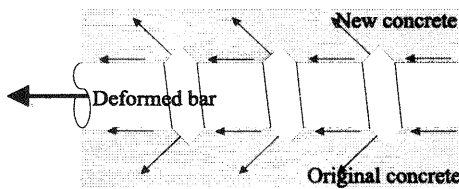
3.1 Numerical modeling

The specimen was analyzed using the two dimensional smeared crack model developed by Uchida et al. to study the crack propagation process. The concept of the fictitious crack model is embedded in their smeared crack model. The interface was modeled as a unique layer of concrete with less G_F value than that of the surrounding concrete. The reduction factor of G_F for the interface concrete element was dependent on the interface condition and determined so that the maximum bond strength were consistently predicted for specimens with different concrete strengths.

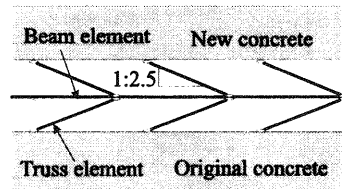
Mesh design for the concrete is shown in Fig. 6. Constant strain triangles were used assuming a plane stress condition. White circles represent

Table 4. Parameters used in the analysis and results

Specimen	Concrete representing the interface		Elsewhere		τ_{FEM} (MPa)	τ_{exp} (MPa)	$\frac{\tau_{FEM}}{\tau_{exp}}$
	σ_t (MPa)	G_F (N/mm)	σ_t (MPa)	G_F (N/mm)			
30-30M	-	-	5.62	0.225	3.44	3.36	1.02
30-30P	2.25	0.090	Ditto	Ditto	1.86	2.29	0.18
30-30R	4.50	0.180	Ditto	Ditto	2.99	2.85	1.05
45-45M	-	-	7.32	0.293	4.14	4.11	1.01
45-45P	2.93	0.117	Ditto	Ditto	2.20	2.35	0.94
45-45R	5.86	0.234	Ditto	Ditto	3.63	3.47	1.05
70-70M	-	-	9.72	0.389	5.00	7.41	0.67
70-70P	3.89	0.156	Ditto	Ditto	2.84	2.78	1.02
70-70R	7.78	0.311	Ditto	Ditto	4.38	4.01	1.09
100-100M	-	-	13.26	0.530	6.07	7.72	0.79
100-100P	5.30	0.212	Ditto	Ditto	3.53	-	-
100-100R	10.61	0.424	Ditto	Ditto	5.36	-	-



(a) Interaction between a steel bar and concrete



(b) Beam-truss assemblage

Fig. 8. Modeling a deformed steel bar

roller supports. At the location of the D25 bar, the concrete thickness was reduced to 64 mm whereas elsewhere it was 88 mm. The relation used between closing stress and crack width is shown in Fig. 7. Values σ_t , ω , and G_F for the specimens analyzed are shown in Table 4. Values σ_t are twice as large as the measured tensile strength in Table 2 since a high value of σ_t was necessary to correctly predict the bond strength. This is probably due to the two dimensional modeling. In two dimensional modeling, the external force applied to the D25 bar is resisted by the concrete in the inplane direction only. However, the external force is in reality resisted by the stress in the out-of-plane direction as well. Since this out-of-plane resistance was neglected, the resistance for the two dimensional elements had to be artificially raised. It is anticipated that as long as the two dimensional modeling

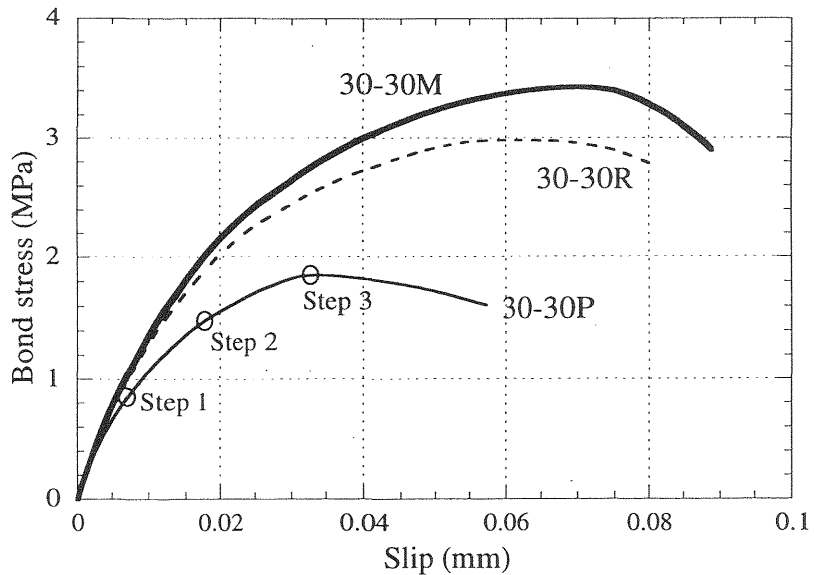
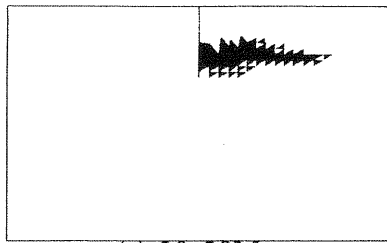


Fig. 9. Bond stress and slip relations obtained in numerical analysis

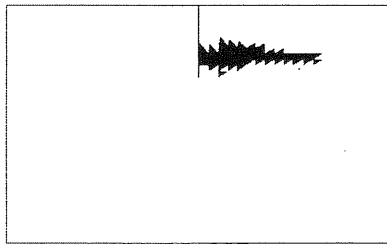
is used, σ_t needs to be changed if the geometry of the specimen is different. In the smeared crack model used in this analysis, the value ω was converted to strain by dividing by the characteristic length of the element, which is the projected length of the element perpendicular to the crack direction. For this analysis, concrete was taken as cracked only when the maximum principal strain exceeds the critical strain for each element.

The interface was modeled by inserting a unique layer of elements at the interface location. Values σ_t were reduced to 80 % for R type and 40% for P type, specimens. Since ω was fixed, G_F was also reduced by the same amount for each type of specimen. The same reduction factor was used for specimens with the same interface condition. Those values were determined so that the maximum bond strength were consistently predicted for specimens with different concrete strengths.

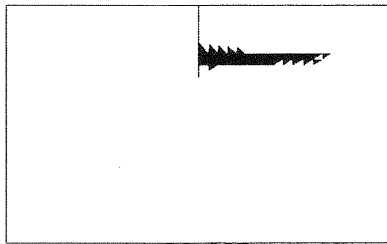
Stress transfer from the D25 bar to the surrounding concrete was modeled using a beam-truss assemblage as shown in Fig. 8. The interaction between the D25 bar and the concrete was modeled as in Fig. 8(a). The D25 bar transfers forces in the shear and radial directions and those actions were



(a) 30-30M

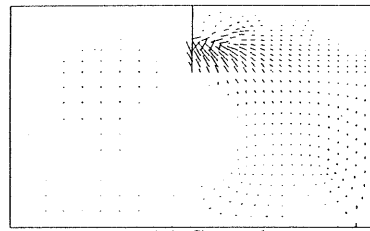


(b) 30-30R

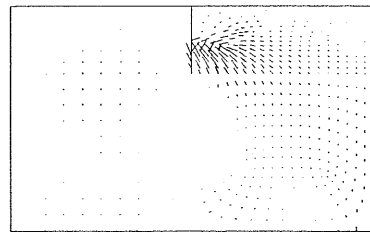


(c) 30-30P

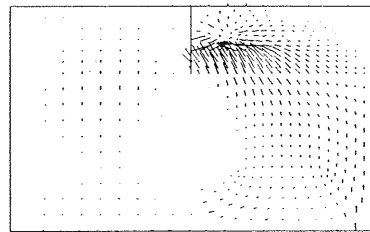
Fig. 10. Elements whose principal strain exceeded the cracking strain at the peak load



(a) Step 1



(b) Step 2



(c) Step 3

Fig. 11. Magnitude and direction of the principal stress for 30-30P

modeled with the beam-truss assemblage shown in Fig. 8(b). The beam elements had the same bending and axial stiffness as the D25 bar. The nodes of the beam elements were connected to the nodes shown as black circles in Fig. 6 by truss elements. The angle of these truss elements was fixed at 1:2.5. The beam and truss assembly represents the shear and wedging action when the beam elements move horizontally. To load the specimen, the displacement was applied incrementally to the beam element at the slit location as shown by the arrow in Fig. 6.

3.2 Analytical results

Analyses were carried out for specimens whose nominal strength for the original concrete was the same as that of the new concrete. Bond stress and slip relations are shown in Fig. 9 for three specimen types whose nominal concrete strength is 30 MPa. Slip is the relative horizontal displacement of the D25 bar to the surrounding concrete at the slit location. Unfortunately the experimental data cannot be used for comparison as stated in 2.3. All three curves show that the stiffness reduces gradually as the slip increases and the bond stress reaches a maximum before the slip reaches 0.1 mm.

The predicted bond strengths for 12 specimen types are listed together with experimental values in Table 4. They are also compared with the experimental values in Fig. 5. Specimen 30-30P and monolithic specimens with high strength concrete (70-70M and 100-100M) have large errors but the results are good for the rest of the specimens. The relation between closing pressure and crack width needs to be modified to predict the high experimental results for 70-70M and 100-100M. However, values for σ_t and G_F are already high and failure modes may need to be closely examined in the experiment for further analysis.

For the three specimen types shown in Fig. 9, the elements which exceeded the cracking strain at the peak bond stress are shown in black in Fig. 10. It can be seen that damage concentrated more at the interface for P type specimens than for M and R type specimens.

For the 30-30P type specimen, the direction and magnitude of the principal stress for each concrete element are shown in Fig. 11. The three steps in Fig. 11 correspond to the same number in Fig. 9. As the bond stress increases, the location of the larger principal stress moves from the tip of the slit to the right along the interface.

4. Conclusions

1. Although the relative displacement between a deformed steel bar and the surrounding concrete is a critical factor for studying bond characteristics, it is difficult to determine displacement experimentally. Precise measurements would enhance understanding of bond.
2. The smeared crack model was able to predict the bond strength for a specimen with the interface but the model needs to be refined to correctly predict the maximum bond stress for monolithic specimens with concrete strength more than 70 MPa. In this prediction, the maximum principal strain was taken as the cracking criteria.
3. The interface was modeled as a layer of weaker concrete elements. This simple modeling was able to predict the bond splitting behavior.

Acknowledgment

The finite element program used in this study was originally developed by Prof. Yuichi Uchida at Gifu University. The authors would like to acknowledge Y. Tsujimoto and R. Isowaki for their great contributions to the computational analysis.

References

- Dahlblom, O. and Ottosen, N. S. (1990) Smearred Crack Analysis Using Generalized Fictitious Crack Model. **Journal of Engineering Mechanics, ASCE**, 116(1), 55-76.
- Feenstra, P. H. (1993) **Computational Aspects of Biaxial Stress in Plain and Reinforced Concrete**, Ph. D. Thesis, Dept. of Civil Engrg., Univ. Illinois at Urbana-Champaign.
- Hillerborg, A., Modeer, M. and Pertersson, P.E. (1976) Analysis of Crack Formation and Crack Growth in Concrete by Means of Fracture Mechanics and Finite Elements, **Cement and Concrete Research**, 6, 773-782.
- Kono, S., Hawkins, N. M. and Kobayashi, A. S. (1995) Concrete Design and Fracture Mechanics Concepts to predict the shear strength of concrete structures, in **Proc. FRAMCOS-2**, Aedificatio publisher, ed. F.H. Wittmann, III, 1707-1720.
- Kono, S. (1995) **Mixed Mode Fracture of Concrete**, Ph. D. Thesis, Dept. of Civil Engrg., Univ. Illinois at Urbana-Champaign.
- Rots, J.G. (1988) **Computational Modeling of Concrete Fracture**, Ph. D. Thesis, Delft University of Technology.
- Shah, S., Swartz, S. E. and Ouyang, C. (1995) **Fracture mechanics of concrete**. John Wiley & Sons, Inc.
- Uchida, Y., Rokugo, K. and Koyanagi, W. (1993) FE analysis of crack propagation in plain concrete using smeared crack model with concept of fictitious crack model. **Journal of Japan society of civil engineering**, 466(19), 89-96.